Journal of Physics: Conference Series **335** (2011) 012038 doi:10.1088/1742-6596/335/1/012038

Angular analysis of $B \to V(\to P_1 P_2) + \bar{\ell}\ell$ decays

Christoph Bobeth[1,3], Gudrun Hiller[2] and Danny van Dyk[2]

[1] Institute of Advanced Study & Excellence Cluster Universe, Technische Universität München, D-85748 Garching, Germany

[2] Institut für Physik, Technische Universität Dortmund, D-44221 Dortmund, Germany

E-mail: christoph.bobeth@ph.tum.de

Abstract. The angular analysis of exclusive rare B-meson decays via intermediate vector mesons V into 4-body final states of two pseudo-scalars P_1, P_2 and a pair of light leptons $\ell = e, \mu$ offers a large set of observables. They can be used to test the electroweak short-distance couplings in the Standard Model and to search for New Physics. The two kinematic regions of low and high dilepton mass depend on short-distance physics in complementary ways and can be expanded in powers of $\Lambda_{\rm QCD}/m_b$. These expansions guide towards suitable combinations of observables allowing to *i*) reduce the hadronic uncertainties in the extraction of the short-distance couplings or *ii*) test the lattice QCD $B \to V$ form factors in short-distance independent combinations. Several such possibilities of CP-averaged and CP-asymmetric (T-even and T-odd) quantities are presented for $\bar{B}^0_d \to \bar{K}^{*0}(\to K^-\pi^+) + \bar{\ell}\ell$ and time-integrated CP-asymmetries without tagging for $\bar{B}_s, B_s \to \phi(\to K^-K^+) + \bar{\ell}\ell$ decays in view of the latest B-factory and CDF results and the forthcoming LHCb measurements.

1. Introduction

The $b \to s + \bar{\ell}\ell$ induced flavour changing neutral current (FCNC) decays of the B-meson are well known to provide sensitive probes of the electroweak short-distance couplings of the Standard Model (SM) and to test scenarios beyond (BSM). Hitherto existing experimental results from the B-factory experiments Babar [1] and Belle [2] as well as the Tevatron experiment CDF [3] are in the ballpark of the SM predictions and provide constraints on the couplings $\mathcal{C}_{9,10}$ related to 4-Fermi operators $(\bar{s}\gamma_\mu P_L b)\,(\bar{\ell}\gamma^\mu\{1,\gamma_5\}\ell)$ [4, 5]. Further experimental progress is expected soon from the final analysis of the full data sets of Babar and Belle, as well as the CDF one with at least doubled statistics. Eventually, LHCb will dominate statistically for final states containing charged particles only, already with a rather low luminosity of a few fb^{-1} [6]. The Super-B factories are expected to contribute to $\ell = e$, just as the B-factories do presently.

Especially the angular analysis of the 4-body final state of $B \to V(\to P_1 P_2) + \bar{\ell}\ell$ decays offers a large number of observables in the fully differential distribution [7, 8]. Here the intermediate V is assumed to be on-shell in the narrow-resonance approximation which restricts the number of kinematic variables to four[4]. Using $\bar{B}^0_d \to \bar{K}^{*0}(\to K^-\pi^+) + \bar{\ell}\ell$ for illustration, they might be chosen as depicted in figure 1.

[3] Speaker

[4] The off-resonance case has been studied in [9].

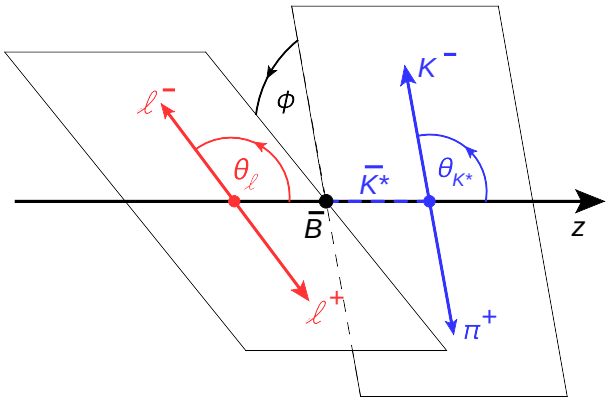

Figure 1. Kinematic variables of $\bar{B}^0_d \to \bar{K}^{*0}(\to K^-\pi^+) + \bar{\ell}\ell$ decays: *i*) the $(\bar{\ell}\ell)$-invariant mass squared q^2, *ii*) the angle θ_ℓ between $\ell = \ell^-$ and $\bar{B}$ in the $(\bar{\ell}\ell)$ center of mass (c.m.), *iii*) the angle θ_{K^*} between K^- and $\bar{B}$ in the $(K^-\pi^+)$ c.m. and *iv*) the angle ϕ between the two decay planes spanned by the 3-momenta of the $(K\pi)$- and $(\bar{\ell}\ell)$-systems, respectively.

The differential decay rate, after summing over lepton spins, factorises into

$$\begin{aligned}\frac{8\pi}{3}\frac{d^4\Gamma}{dq^2\, d\cos\theta_\ell\, d\cos\theta_{K^*}\, d\phi} &= J_1^s \sin^2\theta_{K^*} + J_1^c \cos^2\theta_{K^*} + (J_2^s \sin^2\theta_{K^*} + J_2^c \cos^2\theta_{K^*})\cos 2\theta_\ell \\ &+ J_3 \sin^2\theta_{K^*}\sin^2\theta_\ell \cos 2\phi + J_4 \sin 2\theta_{K^*}\sin 2\theta_\ell \cos\phi + J_5 \sin 2\theta_{K^*}\sin\theta_\ell\cos\phi \\ &+ (J_6^s \sin^2\theta_{K^*} + J_6^c \cos^2\theta_{K^*})\cos\theta_\ell + J_7 \sin 2\theta_{K^*}\sin\theta_\ell \sin\phi \\ &+ J_8 \sin 2\theta_{K^*}\sin 2\theta_\ell \sin\phi + J_9 \sin^2\theta_{K^*}\sin^2\theta_\ell \sin 2\phi, \quad (1)\end{aligned}$$

that is, into q^2-dependent observables[5] $J_i^j(q^2)$ and the dependence on the angles θ_ℓ, θ_{K^*} and ϕ. No additional angular dependencies can be induced by any extension of the SM operator basis [11] as found by [12, 13]. The following simplifications arise in the limit $m_\ell \to 0$: $J_1^s = 3J_2^s$, $J_1^c = -J_2^c$ and $J_6^c = 0$.

The differential decay rate $d^4\bar{\Gamma}$ of the CP-conjugated decay $B^0_d \to K^{0*}(\to K^+\pi^-) + \bar{\ell}\ell$ is obtained through the following replacements

$$J^j_{1,2,3,4,7} \to \bar{J}^j_{1,2,3,4,7}[\delta_W \to -\delta_W], \qquad J^j_{5,6,8,9} \to -\bar{J}^j_{5,6,8,9}[\delta_W \to -\delta_W], \quad (2)$$

due to $\ell \leftrightarrow \bar{\ell} \Rightarrow \theta_\ell \to \theta_\ell - \pi$ and $\phi \to -\phi$. The CP-violating (weak) phases δ_W are conjugated.

The angular distribution provides twice as many observables (J_i^j and $\bar{J}_i^j$) when the decay and its CP-conjugate decay are measured separately. This doubles again if the $\ell = e$ and μ lepton flavours are not averaged. Notably, CP-asymmetries can be measured in an untagged sample of B-mesons due to the presence of CP-odd observables ($i = 5, 6, 8, 9$) [7]. Moreover, T-odd observables $\sim \cos\delta_s \sin\delta_W$ ($i = 7, 8, 9$) are especially sensitive to weak BSM phases δ_W [10, 14] contrary to T-even ones $\sim \sin\delta_s \sin\delta_W$ ($i = 1, \ldots, 6$), since the CP-conserved (strong) phase δ_s is often predicted to be small. Note, that in the SM CP-violating effects in $b \to s$ are doubly-suppressed by the Cabibbo angle as $\mathrm{Im}[V_{ub}V_{us}^*/(V_{tb}V_{ts}^*)] \approx \bar{\eta}\lambda \sim 10^{-2}$.

The observables J_i^j are bilinear in the transversity amplitudes $A_a^{L,R}$ ($a = 0, \perp, \parallel$ in the limit $m_\ell \to 0$[6]) [15]. Here L, R refer to the chirality of the lepton current. The kinematic dependence on the lepton mass is suppressed by m_ℓ^2/q^2. Hence, non-negligible effects from finite lepton masses at $q^2 > 1$ GeV^2 arise only in BSM scenarios, as for example in the MSSM at large $\tan\beta$ due to neutral Higgs boson exchange, see for instance [16].

Depending on q^2, present theoretical predictions suffer from long-distance dominated $(\bar{q}q)$-resonance background ($q = u, d, s, c$) induced by current-current- and QCD-penguin-operators of

[5] Possibilities to extract q^2-integrated J_i^j from single-differential distributions in θ_ℓ, θ_{K^*} or ϕ can be found in [10].
[6] Two more amplitudes contribute for $m_\ell \neq 0$: A_t (time-like) and in the presence of scalar operators, A_S [12].

the $\Delta B = 1$ effective Hamiltonian. Compared to the leading c-current-current contribution, the u-current-current one is suppressed by small CKM elements and the QCD-penguin contribution by small Wilson coefficients. The light (u, d, s)-resonances affect the FCNC $b \to s + \bar{\ell}\ell$ decay at very low $q^2 \lesssim 1$ GeV^2. The narrow $(\bar{c}c)$-resonances J/ψ and ψ' are vetoed in the experimental analysis, while the broader $(\bar{c}c)$-resonances appear at $q^2 > 14$ GeV^2.

This singles out a low-q^2 and a high-q^2 window which are usually chosen in the intervals $q^2 \in [1, 6]$ GeV^2 and $q^2 > 14$ GeV^2, respectively. They correspond to large and low recoil of the K^*-meson, as indicated by the scaling of its energy in the B-meson rest frame: $E_{K^*} \sim m_b/2$ versus $E_{K^*} \sim m_{K^*} + \Lambda_{\rm QCD}$. The heavy quark limit is combined at large recoil with the large energy limit as an application of QCD factorisation (QCDF) [17, 18] whereas at low recoil an operator product expansion (OPE) can be performed [19, 20] in combination with HQET form factor relations [21]. Revealing the symmetries of QCD dynamics in both regions, the expansions reduce the number of hadronic matrix elements. Many works have been inspired in the past decade in order to exploit these symmetries to reduce the hadronic uncertainties in the exclusive decays. Particularly, the angular analysis of the 4-body decay $B \to V(\to P_1 P_2) + \bar{\ell}\ell$ proved most fruitful. For comparison, $B \to P + \bar{\ell}\ell$ decays offer only two additional observables beyond the branching ratio, the lepton forward-backward asymmetry $A_{\rm FB}^{\ell}$ and the flat term F_H^{ℓ} [16].

2. $\bar{\mathbf{B}}_{\mathbf{d}}^{\mathbf{0}} \to \bar{\mathbf{K}}^{\mathbf{0}*}(\to \mathbf{K}^- \pi^+) + \bar{\ell}\ell$

The experimental situation in regard to lepton final states is twofold: On the one hand, the (Super-) B-factories are able to measure both $\ell = e$ and μ modes separately. On the other hand, most detectors at hadronic collider machines prefer $\ell = \mu$, however, LHCb might be able to study $\ell = e$, too [22].

2.1. Low-q^2 / Large recoil region

Using QCDF in the low-q^2 region, the seven $B \to V$ QCD form factors $(V, A_{0,1,2}, T_{1,2,3})$ reduce to two universal form factors $\xi_{\perp,\parallel}$ [23]. Furthermore, the $B \to K^* + \bar{\ell}\ell$ amplitudes factorise [17, 18][7], where the numerically leading contributions to the transversity amplitudes are [15]

$$A_{\perp,\parallel}^{L,R} \propto \pm c_{\perp}^{L,R} \times \xi_{\perp}, \qquad\qquad A_0^{L,R} \propto c_{\parallel}^{L,R} \times \xi_{\parallel}, \tag{3}$$

with short-distance coefficients $c_{\perp,\parallel}^{L,R}$. The transversity amplitudes have been used to construct the observables $A_T^{(2)}$ [15] and $A_T^{(3,4,5)}$ [26, 27] with reduced hadronic uncertainties and an improved sensitivity to the chirality flipped operators $\mathcal{O}'_{7,9,10}$. Instead of fitting the observables J_i^j from the angular distribution, the authors of reference [26, 27] pursue the possibility to fit directly the transversity amplitudes which necessitates the identification of their rephasing properties. Moreover, the authors investigate the experimental reconstruction uncertainties of their method at LHCb, including among the theoretical uncertainties also lacking subleading QCDF contributions by simple power counting.

The original analysis of the CP asymmetries of the rate $A_{\rm CP}$ and the angular coefficients [7]

$$A_i \equiv \frac{2\big(J_i^j - \bar{J}_i^j\big)}{d(\Gamma + \bar{\Gamma})/dq^2} \quad \text{for } i = 3, 6, 9, \qquad\qquad A_i^D \equiv \frac{-2\big(J_i^j - \bar{J}_i^j\big)}{d(\Gamma + \bar{\Gamma})/dq^2} \quad \text{for } i = 4, 5, 7, 8 \tag{4}$$

based on naive factorisation was extended using QCDF to the low-q^2 region by taking into account the NLO QCD corrections for the strong phase δ_s [10]. Both $A_{3,9}$ vanish in the SM at leading order in QCDF since they are proportional to the interference of SM and

[7] One might use equivalently soft collinear effective theory (SCET) [24, 25].

Table 1. The SM predictions of the q^2-integrated CP-asymmetries of $\bar{B}^0_d \to \bar{K}^{0*}(\to K^-\pi^+) + \bar{\ell}\ell$ decays ($q^2 \in [1,6]$ GeV^2) and their relative uncertainties from the form factors $\xi_{\perp,\parallel}$ and the renormalisation scale μ_b [10] (see also [12]). Also shown are the ranges of the CP asymmetries after applying the experimental constraints at 90 % C.L. for the generic model-independent BSM scenario [10]. Note that the SM predictions are given in units of 10^{-3}.

		$\langle A_{\rm CP}\rangle$	$\langle A_3\rangle$	$\langle A_4^D\rangle$	$\langle A_5^D\rangle$	$\langle A_6\rangle$	$\langle A_7^D\rangle$	$\langle A_8^D\rangle$	$\langle A_9\rangle$
SM	$\times 10^{-3}$	$4.2^{+1.7}_{-2.5}$	-	$-1.8^{+0.3}_{-0.3}$	$7.6^{+1.5}_{-1.6}$	$-6.4^{+2.2}_{-2.7}$	$-5.1^{+2.4}_{-1.6}$	$3.5^{+1.4}_{-2.0}$	-
	$\xi_{\perp,\parallel}$[%]	$^{+19}_{-24}$	-	$^{+11}_{-8}$	$^{+10}_{-13}$	$^{+31}_{-39}$	$^{+11}_{-8}$	$^{+7.4}_{-10}$	-
	μ_b[%]	$^{+33}_{-51}$	-	$^{+2}_{-6}$	$^{+7}_{-8}$	$^{+0}_{-2}$	$^{+42}_{-26}$	$^{+37}_{-53}$	-
BSM	max	+0.10	+0.08	+0.04	+0.07	+0.11	+0.76	+0.48	+0.60
	min	−0.12	−0.08	−0.04	−0.07	−0.13	−0.76	−0.48	−0.62

chirality flipped operators, making them ideal probes of the latter. Furthermore, $A^D_{7,8}$ are subject to cancellations at leading order in QCD, such that the NLO QCD corrections give large corrections. The q^2-integrated SM predictions of the CP asymmetries are summarised in table 1. They are, as expected, tiny and below a percent. A model-independent analysis in the presence of the BSM contributions to the SM and the chirality flipped operators $\mathcal{O}'_{7,9,10}$ shows substantial room for enhancement. The T-odd asymmetries $A^D_{7,8,9}$ can be of order one. However, the experimental uncertainties at LHCb are large for CP-asymmetries, even when considering improved normalisations as discussed for A^{V2s}_{6s} and A^V_8 [27].

The rate-normalised CP-averaged quantities $S^j_i \sim (J^j_i + \bar{J}^j_i)$ constitute another important set of observables, of which the CP-odd ones ($i = 5,6,8,9$) require B-tagged samples. The S^j_i have been analysed in the SM, model-independently and model-dependently in great detail [12, 13]. Especially, the lepton forward-backward asymmetry $A_{\rm FB}$ (related to S^s_6) and S_5 could be measured rather precisely with early LHCb data of 2 fb^{-1} [28].

It should be noted that [26, 27] estimate uncertainties due to unknown subleading $\mathcal{O}(\Lambda_{\rm QCD}/E_{K^*})$ contributions to both form factors and $B \to K^* + \bar{\ell}\ell$ amplitudes by power counting. Contrary, [12] does not make use of the large recoil symmetry relations of the form factors in the LO QCD contribution of the said amplitudes. Instead, all seven QCD form factors determined from light cone sum rules (LCSR) [29] are used, thus accounting for the associated unknown subleading $\mathcal{O}(\Lambda_{\rm QCD}/E_{K^*})$ contributions. The direct application of the LCSR results reduces the form factor uncertainties [12] due to more efficient cancellations.

Recently, soft-gluon emission effects due to $(\bar{c}c)$-resonances were found to extend down to the low-q^2 region [30] affecting the q^2-differential rate at most about +15 % at $q^2 = 6$ GeV^2. Due to this relatively large shift such effects should be investigated further and should be considered in future studies of the exclusive rare decays.

2.2. High-q^2 / Low recoil region

Assuming quark-hadron duality, the low recoil region can be studied using an OPE in combination with HQET to treat the long-distance contributions from current-current and QCD-penguin operators [19, 20]. The authors of [20] perform the OPE without subsequent matching to HQET contrary to [19], among further technical details. Duality violating corrections to the OPE are estimated in [20] and found to be small. In [19] it is shown, that at the leading order in the

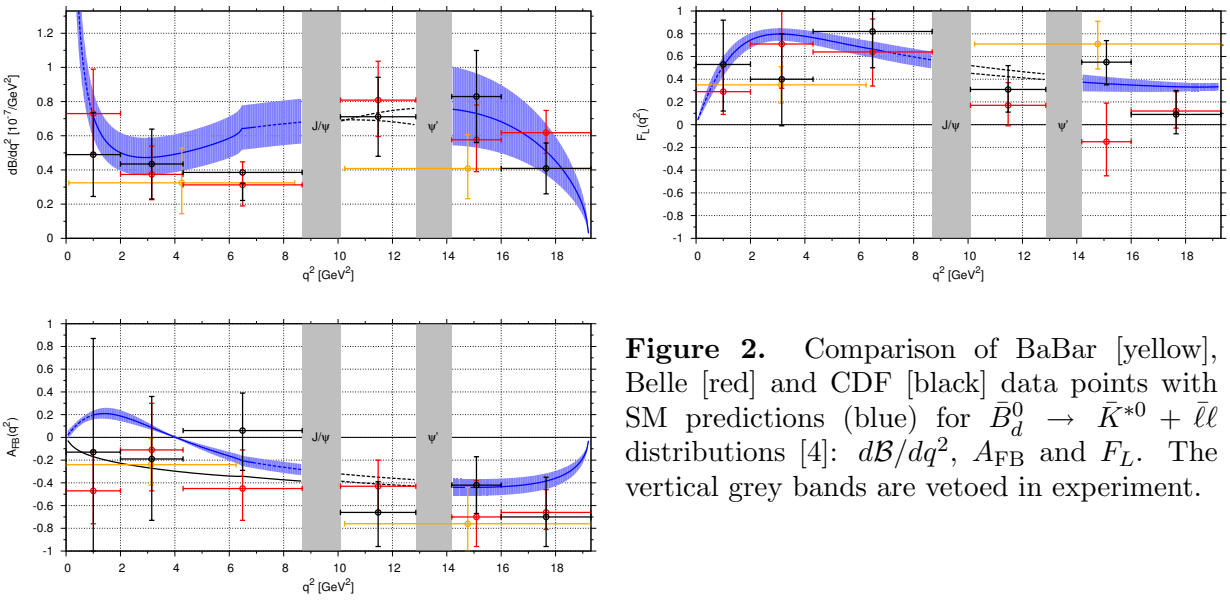

Figure 2. Comparison of BaBar [yellow], Belle [red] and CDF [black] data points with SM predictions (blue) for $\bar{B}^0_d \to \bar{K}^{*0} + \bar{\ell}\ell$ distributions [4]: $d\mathcal{B}/dq^2$, $A_{\rm FB}$ and F_L. The vertical grey bands are vetoed in experiment.

$\Lambda_{\rm QCD}/Q$, $Q = \{\sqrt{q^2}, m_b\}$ expansion[8] all hadronic matrix elements can be expressed through the 3 QCD form factors $V, A_{1,2}$. As a consequence, a universal short-distance dependence emerges for all transversity amplitudes ($a = 0, \perp, \|$) [4]

$$A_a^{L,R} \propto c_{L,R} \times f_a, \qquad c_{L,R} = (\mathcal{C}_9^{\rm eff} \mp \mathcal{C}_{10}) + \kappa \frac{2m_b}{q^2} \mathcal{C}_7^{\rm eff}, \tag{5}$$

with the (effective) short-distance couplings $\mathcal{C}^{\rm eff}_{7,9,10}$ and the form factor terms f_a ($a = 0, \perp, \|$) which are linear in $V, A_{1,2}$. The factor $\kappa \sim 1$ is known including NLO in QCD from matching QCD onto HQET [19]. The term $\propto \mathcal{C}_7^{\rm eff}$ is subject to uncertainties of order $\Lambda_{\rm QCD}/m_b$ due to the HQET form factor relations, which are additionally suppressed in the SM by $|\mathcal{C}_7/\mathcal{C}_9| \sim 0.1$. As a consequence of (5) $J_7 = J_8 = J_9 = 0$ and the remaining angular observables

$$\begin{aligned} &J_2^c \sim U_1 = 2\rho_1 f_0^2, \qquad (2J_2^s + J_3) \sim U_2 = 2\rho_1 f_\perp^2, \qquad (2J_2^s - J_3) \sim U_3 = 2\rho_1 f_\|^2, \\ &J_4 \sim U_4 = 2\rho_1 f_0 f_\|, \qquad J_5 \sim U_5 = 4\rho_2 f_0 f_\perp, \qquad J_6^s \sim U_6 = 4\rho_2 f_\| f_\perp, \end{aligned} \tag{6}$$

depend only on the two short-distance (dominated) combinations $\rho_1 = (|c_R|^2 + |c_L|^2)/2$ and $\rho_2 = (|c_R|^2 - |c_L|^2)/4$ [4]. From (6) one obtains the three long-distance free ratios

$$H_T^{(1)} = \frac{U_4}{\sqrt{U_1 \cdot U_3}} = 1, \qquad H_T^{(2)} = \frac{U_5}{\sqrt{U_1 \cdot U_2}} = 2\,\frac{\rho_2}{\rho_1}, \qquad H_T^{(3)} = \frac{U_6}{\sqrt{U_2 \cdot U_3}} = 2\,\frac{\rho_2}{\rho_1}. \tag{7}$$

After integration over $q^2 \in [14.0, 19.2]$ GeV^2 one obtains in the SM

$$\langle H_T^{(1)} \rangle = +0.997 \pm 0.003, \qquad \langle H_T^{(2)} \rangle = -0.972 \pm 0.010, \qquad \langle H_T^{(3)} \rangle = -0.958 \pm 0.010. \tag{8}$$

Details concerning the definition of $\langle \ldots \rangle$ and the theoretical uncertainties are given in [4] as well as the results for $\mathcal{B}, A_{\rm FB}, F_L$ and $A_T^{(2,3,4)}$. We stress that $\langle H_T^{(1)} \rangle \approx 1$ holds model-independently.

[8] Note, that the subleading order is additionally suppressed by α_s.

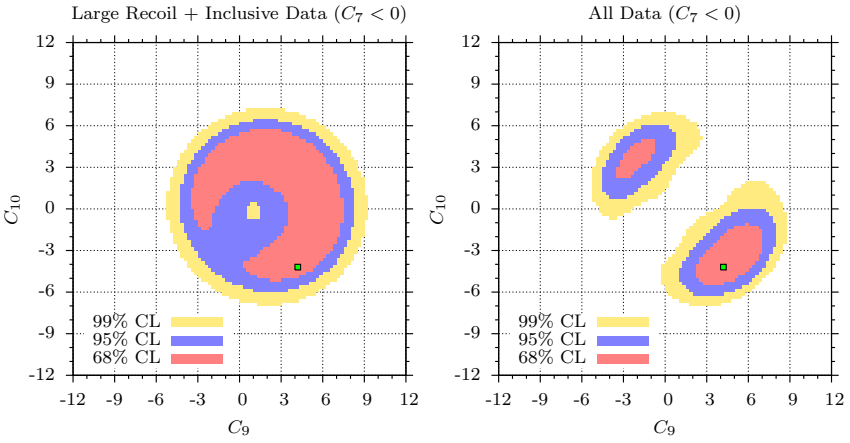

Figure 3. Constraints on real-valued $\mathcal{C}_{9,10}$ at 68%, 95% and 99% CL from low-q^2 bins of $\bar{B}^0_d \to \bar{K}^{*0}\bar{\ell}\ell$ and $B \to X_s\bar{\ell}\ell$ [left] and when adding high-q^2 bins [right] [4, 5]. Here $\mathcal{C}_7 = +\mathcal{C}_7^{\rm SM}$ is fixed. The square marks the SM value of $(\mathcal{C}_9, \mathcal{C}_{10})$.

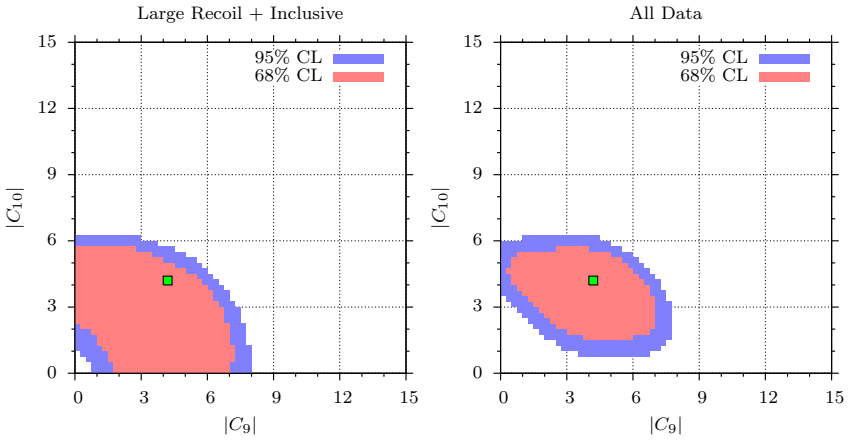

Figure 4. Constraints on $|\mathcal{C}_{9,10}|$ at 68% and 95% CL for complex-valued $\mathcal{C}_{9,10}$ from low-q^2 bins of $\bar{B}^0_d \to \bar{K}^{*0}\bar{\ell}\ell$ and $B \to X_s\bar{\ell}\ell$ [left] and when adding high-q^2 bins [right] (see [5] for details). The square marks the SM value of $(\mathcal{C}_9, \mathcal{C}_{10})$.

Hence, deviations from this prediction test the validity of the OPE framework. Furthermore, the following short-distance free ratios

$$\frac{f_0}{f_\parallel} = \sqrt{\frac{U_1}{U_3}} = \frac{U_1}{U_4} = \frac{U_4}{U_3} = \frac{U_5}{U_6}, \qquad \frac{f_0}{f_\perp} = \sqrt{\frac{U_1}{U_2}}, \qquad \frac{f_\perp}{f_\parallel} = \sqrt{\frac{U_2}{U_3}} = \frac{\sqrt{U_1 U_2}}{U_4} \tag{9}$$

allow to test the $B \to V$ form factors at high-q^2, such as obtained from lattice QCD, using experimental data [4].

A comparison of the SM predictions and the available data from BaBar, Belle and CDF for low- and high-q^2 regions is shown in figure 2 where the main uncertainties (shaded bands) arise from the form factors and the missing subleading corrections of order $\Lambda_{\rm QCD}/m_b$ as estimated by power counting [4]. The Belle and CDF measurements of the three low- and high-q^2 bins $q^2 \in [1,6], [14.18, 16.0], [16.0, 19.21]$ GeV^2 of $\mathcal{B}$ and $A_{\rm FB}$ (and $q^2 \in [1,6]$ GeV^2 of F_L) yield the first constraints on the short-distance couplings $\mathcal{C}_{9,10}$ of the SM operators $\mathcal{O}_{9,10}$ beyond naive factorisation. The constraints for real-valued $\mathcal{C}_{9,10}$ are shown in figure 3 fixing $\mathcal{C}_7 = +\mathcal{C}_7^{\rm SM}$ (results for $\mathcal{C}_7 = -\mathcal{C}_7^{\rm SM}$ are available in [4]) when employing low-q^2 data only and when adding high-q^2 data[9], respectively. Figure 4 shows $|\mathcal{C}_{10}|$ vs. $|\mathcal{C}_9|$ for complex-valued $\mathcal{C}_{9,10}$ and results of (ϕ_9 vs. $|\mathcal{C}_9|$), (ϕ_{10} vs. $|\mathcal{C}_{10}|$) and (ϕ_{10} vs. ϕ_9) can be found in [5]. Both figures demonstrate the strong constraining power of the high-q^2 region on $\mathcal{C}_{9,10}$, and consistency with low-q^2 data.

CP asymmetries with improved short-distance sensitivity can be designed in analogy to $H_T^{(1,2,3)}$, since $\bar{J}_i^j \sim \bar{\rho}_a$ with $\bar{\rho}_a = \rho_a[\delta_W \to -\delta_W]$. It is convenient to consider the three

[9] Using an extrapolation of the $B \to V$ form factors from low-q^2 QCD LCSR [29].

CP-asymmetries

$$a_{\rm CP}^{(1)} = \frac{\rho_1 - \bar\rho_1}{\rho_1 + \bar\rho_1}, \qquad a_{\rm CP}^{(2)} = \frac{\frac{\rho_2}{\rho_1} - \frac{\bar\rho_2}{\bar\rho_1}}{\frac{\rho_2}{\rho_1} + \frac{\bar\rho_2}{\bar\rho_1}}, \qquad a_{\rm CP}^{(3)} = 2\,\frac{\rho_2 - \bar\rho_2}{\rho_1 + \bar\rho_1}, \tag{10}$$

with various possibilities to measure them [5]. Moreover, $a_{\rm CP}^{(3)}$ can be extracted from an untagged B-meson sample. There are no T-odd CP-asymmetries at low-recoil due to (6): $J_{7,8,9} = 0$. In the SM $|a_{\rm CP}^{(1,2,3)}|_{\rm SM} \lesssim 10^{-4}$ whereas a model-independent analysis for complex-valued $\mathcal{C}_{9,10}$ allows values up to $|\langle a_{\rm CP}^{(1,3)}\rangle| \lesssim 0.2$ and $|\langle a_{\rm CP}^{(2)}\rangle|$ is presently unconstrained (see [5] for details).

3. CP asymmetries without tagging

The decays $\bar B_s, B_s \to \phi(\to K^-K^+) + \bar\ell\ell$ require to account for the mixing of the initial $\bar B_s^0$- and B_s^0-mesons before decaying into the common final state. Consequently, their observables depend additionally on the $\bar B_s - B_s$ mixing phase Φ_s and the lifetime difference $\Delta\Gamma_s$, which are currently being analysed at the Tevatron, for instance in $\bar B_s, B_s \to \phi(\to K^+K^-) + J/\psi(\to \bar\ell\ell)$. In this respect, the CP-odd property of the observables J_i^j with $i = 5, 6, 8, 9$ allows to measure the associated CP-asymmetries from an untagged and time-integrated data set.

The CP-asymmetries A_i^{mix} for $i = 6, 9$ and A_i^{Dmix} for $i = 5, 8$ have been worked out at low-q^2 [10]. They match the corresponding A_i and A_i^D of the flavour-specific unmixed decays for $\Delta\Gamma_s \to 0$. There the CP-averaged rate has been used as normalisation. An improved cancellation of the hadronic uncertainties might be achieved along the lines of the unmixed case by choosing the normalisations proposed for A_{6s}^{V2s} and A_8^V [27].

At high-q^2 the CP-asymmetries associated with J_i^j, $i = 8, 9$ vanish and those with $i = 5, 6$ can be related to the same short-distance dominated $a_{\rm CP}^{mix}$ using the normalisations as indicated in reference [5]. Notably, $a_{\rm CP}^{mix}$ is independent of the sign of $\Delta\Gamma_s$ and the dependence on Φ_s is rather weak for small $\Delta\Gamma_s/\Gamma_s$. Experimentally, $\Delta\Gamma_s/\Gamma_s \sim \mathcal{O}(0.1)$.

4. Conclusion

The angular analysis of the exclusive $\bar B_d^0 \to \bar K^{0*}(\to K^-\pi^+) + \bar\ell\ell$ and $\bar B_s, B_s \to \phi(\to K^-K^+) + \bar\ell\ell$ decays with 4-body final states offers a rich phenomenology to test the short-distance flavour couplings in a large number of observables. The LHCb experiment is expected to improve the experimental situation tremendously in the near future, but also the upcoming final analysis of the complete BaBar, Belle and CDF data sets will contribute to the exploration of the borders of the SM.

The low- and high-q^2 regions are accessible to power expansions which reveal symmetries of QCD and indicate suitable combinations of observables to reduce the hadronic uncertainties. This allows for precise theory predictions for the exclusive decays.

The low-q^2 region is theoretically (QCDF, SCET) well understood and effects of $(\bar cc)$-resonances can be estimated. It offers many interesting observables which wait for confrontation with data.

The high-q^2 region is based on an OPE relying on quark-hadron duality. Violations of the latter could be signaled experimentally by deviations from $H_T^{(1)} = 1$. Currently, the $B \to V$ form factors used at high-q^2 are extrapolated from the low-q^2 region using a dipole formula, but lattice calculations for the high-q^2 regions are in progress [31]. There are two "long-distance free" ratios $H_T^{(2,3)}$ which provide tests of the SM and, moreover, several "short-distance free" ratios which offer direct comparison of the lattice results for ratios of form factors with data.

A new flavour tool "EOS" aimed at the evaluation of the observables covered in this article is developed at TU Dortmund [32] whose first stable release is expected during 2011.

Acknowledgments

C. B. thanks the organisers of the *DISCRETE 2010 - Symposium on Prospects in the Physics of Discrete Symmetries* for the opportunity to present a talk and the kind hospitality in Rome. The work reported here has been supported in part by the Bundesministerium für Bildung und Forschung (BMBF).

References

[1] B. Aubert *et al.* [BABAR Collaboration], Phys. Rev. D **79** (2009) 031102 [arXiv:0804.4412 [hep-ex]].
[2] J. T. Wei *et al.* [BELLE Collaboration], Phys. Rev. Lett. **103** (2009) 171801 [arXiv:0904.0770 [hep-ex]].
[3] T. Aaltonen *et al.* [CDF Collaboration], Phys. Rev. Lett. **106** (2011) 161801 [arXiv:1101.1028 [hep-ex]].
[4] C. Bobeth, G. Hiller and D. van Dyk, JHEP **1007** (2010) 098 [arXiv:1006.5013 [hep-ph]].
[5] C. Bobeth, G. Hiller and D. van Dyk, arXiv:1105.0376 [hep-ph].
[6] B. Adeva *et al.*, [The LHCb Collaboration], LHCb-PUB-2009-029 [arXiv:0912.4179].
[7] F. Kruger, L. M. Sehgal, N. Sinha and R. Sinha, Phys. Rev. D **61** (2000) 114028 [Erratum-ibid. D **63** (2001) 019901] [arXiv:hep-ph/9907386].
[8] C. S. Kim, Y. G. Kim, C. D. Lu and T. Morozumi, Phys. Rev. D **62** (2000) 034013 [arXiv:hep-ph/0001151].
[9] B. Grinstein and D. Pirjol, Phys. Rev. D **73** (2006) 094027 [arXiv:hep-ph/0505155].
[10] C. Bobeth, G. Hiller and G. Piranishvili, JHEP **0807** (2008) 106 [arXiv:0805.2525 [hep-ph]]; PoS **BEAUTY2009** (2009) 047 [arXiv:0911.4054 [hep-ph]].
[11] C. Bobeth, M. Misiak and J. Urban, Nucl. Phys. B **574** (2000) 291 [arXiv:hep-ph/9910220].
[12] W. Altmannshofer, P. Ball, A. Bharucha, A. J. Buras, D. M. Straub and M. Wick, JHEP **0901** (2009) 019 [arXiv:0811.1214 [hep-ph]].
[13] A. K. Alok, A. Datta, A. Dighe, M. Duraisamy, D. Ghosh, D. London and S. U. Sankar, arXiv:1008.2367 [hep-ph].
[14] R. Sinha, arXiv:hep-ph/9608314; C. H. Chen and C. Q. Geng, Nucl. Phys. B **636** (2002) 338 [arXiv:hep-ph/0203003].
[15] F. Kruger and J. Matias, Phys. Rev. D **71** (2005) 094009 [arXiv:hep-ph/0502060].
[16] C. Bobeth, G. Hiller and G. Piranishvili, JHEP **0712** (2007) 040 [arXiv:0709.4174 [hep-ph]].
[17] M. Beneke, T. Feldmann and D. Seidel, Nucl. Phys. B **612** (2001) 25 [arXiv:hep-ph/0106067].
[18] M. Beneke, T. Feldmann and D. Seidel, Eur. Phys. J. C **41** (2005) 173 [arXiv:hep-ph/0412400].
[19] B. Grinstein and D. Pirjol, Phys. Rev. D **70** (2004) 114005 [arXiv:hep-ph/0404250].
[20] M. Beylich, G. Buchalla and T. Feldmann, arXiv:1101.5118 [hep-ph].
[21] B. Grinstein and D. Pirjol, Phys. Lett. B **533** (2002) 8 [arXiv:hep-ph/0201298].
[22] J. Lefrançois and M. H. Schune, LHCb-PUB-2009-008.
[23] M. Beneke and T. Feldmann, Nucl. Phys. B **592** (2001) 3 [arXiv:hep-ph/0008255].
[24] A. Ali, G. Kramer and G. h. Zhu, Eur. Phys. J. C **47** (2006) 625 [arXiv:hep-ph/0601034].
[25] K. S. M. Lee, Z. Ligeti, I. W. Stewart and F. J. Tackmann, Phys. Rev. D **75** (2007) 034016 [arXiv:hep-ph/0612156].
[26] U. Egede, T. Hurth, J. Matias, M. Ramon and W. Reece, JHEP **0811** (2008) 032 [arXiv:0807.2589 [hep-ph]].
[27] U. Egede, T. Hurth, J. Matias, M. Ramon and W. Reece, JHEP **1010** (2010) 056 [arXiv:1005.0571 [hep-ph]].
[28] A. Bharucha and W. Reece, Eur. Phys. J. C **69** (2010) 623 [arXiv:1002.4310 [hep-ph]].
[29] P. Ball and R. Zwicky, Phys. Rev. D **71** (2005) 014029 [arXiv:hep-ph/0412079].
[30] A. Khodjamirian, T. Mannel, A. A. Pivovarov and Y. M. Wang, JHEP **1009** (2010) 089 [arXiv:1006.4945 [hep-ph]].
[31] Z. Liu, S. Meinel, A. Hart, R. R. Horgan, E. H. Muller and M. Wingate, PoS **LAT2009** (2009) 242 [arXiv:0911.2370 [hep-lat]]; arXiv:1101.2726 [hep-ph].
[32] D. van Dyk *et al.*, http://project.het.physik.tu-dortmund.de/eos/.